International Journal of Heat and Mass Transfer 101 (2016) 542–549

Contents lists available at ScienceDirect

International Journal of Heat and Mass Transfer

journal homepage: www.elsevier.com/locate/ijhmt

Quantifying the role of burn temperature, burn duration and skin thickness in an *in vivo* animal skin model of heat conduction

Christine J. Andrews [a], Leila Cuttle [b], Matthew J. Simpson [c,*]

[a] Centre for Children's Burns and Trauma Research, The University of Queensland, Centre for Children's Health Research, South Brisbane, Queensland 4101, Australia
[b] Centre for Children's Burns and Trauma Research, Queensland University of Technology, School of Biomedical Sciences, Institute of Health and Biomedical Innovation at Centre for Children's Health Research, South Brisbane, Queensland 4101, Australia
[c] School of Mathematical Sciences, Queensland University of Technology (QUT), Brisbane 4001, Australia

ARTICLE INFO

Article history:
Received 21 March 2016
Received in revised form 14 May 2016
Accepted 16 May 2016

Keywords:
Thermal injury
Burn model
Heat conduction
Thermal diffusivity

ABSTRACT

To determine the extent to which heat conduction through skin is affected by skin thickness, burn temperature, and burn duration, we perform a suite of experiments using an *in vivo* porcine (pig) model. Fourteen different burn conditions are considered, and each burn condition is replicated at least four times, giving a total of sixty four individual experimental burns. The subdermal temperature within the skin is recorded as a function of time during each experiment. To quantitatively interpret the experimental data, we develop an exact solution of a simplified, depth-averaged, heat equation. Calibrating this solution to the experimental data provide estimates of the effective thermal diffusivity of the skin, α, and the effective thermal loss rate, k. Estimates of α and k are obtained for the fourteen different, clinically relevant, burn conditions. Overall, we find $\alpha = 0.03 \pm 0.02$ mm^2/s (to one significant figure), and is approximately independent of the burn duration, burn temperature, and skin thickness (H). This estimate implies that the time required for thermal energy to diffuse vertically down, through the skin of thicker ($H = 2.27$ mm) and thinner ($H = 1.40$ mm) skinned animals is approximately 170 and 70 s, respectively. We find that $k = 0.002 \pm 0.002$/s (to one significant figure). In summary, our results provide contemporary estimates for the thermal properties of *in vivo* porcine skin, which has broad application to heat transfer modelling investigations of thermal injury prevention and thermal therapy studies.

1. Introduction

Scald burns from accidental exposure to hot liquids are the most common cause of thermal injury in children [1]. These burns are extremely painful, may require prolonged treatment, and can cause scarring [2]. Fundamental knowledge of how heat is conducted through skin is essential to inform the development of burn prevention strategies. One way to improve our understanding of heat conduction in skin is to apply a mathematical model to interpret an experimental data set.

Quality experimental data examining heat conduction in living skin are rare. Most experimental research in this area is conducted with pig skin, because pig skin is anatomically and physiologically similar to human skin [3–7]. The most extensive experimental data set exploring heat conduction in skin is the 1947 study by Henriques and Moritz [8]. They excised skin tissue from pigs and estimated the thermal conductivity, α, of the different layers of non-living, *ex vivo*, skin. Henriques and Moritz [8] also estimated the caloric uptake of pig skin *in vivo* when a metal heat source was applied to the surface of the skin and used this information to provide an estimate of the thermal conductivity for *in vivo* conditions. Their estimates of α for the pig dermis is 0.096 mm^2/s and 0.108–0.288 mm^2/s for *ex vivo* and *in vivo* conditions, respectively. More recent *ex vivo* studies using excised pig skin range from using very thick, 5 mm tissue sections including fat [9], to using extremely thin 30 μm sections of epithelial cells [10], and these studies report values for α of 0.11 mm^2/s and 0.029 mm^2/s, respectively. Unfortunately, it is unclear how these kinds of measurements, using different portions of the skin layers in non-living tissue, translate to the more complex situation in living tissue.

Mathematical models of heat transfer in skin are traditionally based on the Pennes bioheat equation [11–13]. This model is an extension of the standard linear heat equation [14,15] with an additional source term that accounts for thermal energy loss [11,12]. Often the source term is used to represent loss to the blood supply, which is known as perfusion [11–13]. Studies that directly combine mathematical modelling with comprehensive *in vivo*

* Corresponding author.
E-mail address: matthew.simpson@qut.edu.au (M.J. Simpson).

http://dx.doi.org/10.1016/j.ijheatmasstransfer.2016.05.070
0017-9310/

Nomenclature

t	time (s)
x	position (mm)
$T(t)$	average temperature in the tissue layer (°C)
$\Delta T(t)$	change in the average temperature in the tissue layer relative to the initial temperature (°C)
T_w	temperature of the water (°C)
T_s	surface temperature of the skin (°C)
t_d	duration of the burn (s)
T_{ref}	reference temperature for the thermal loss (°C)
H	skin thickness (mm)
k	thermal loss coefficient (/s)
Greek symbols	
α	thermal diffusivity (mm^2/s)
λ	constant in the exact solution of the mathematical model (°C)

experimental data sets are scarce. Most previous mathematical models have been parameterised by extrapolating experimental data from existing literature [16–20], or from experimental data sets that describe a single burn condition only [21,22]. In contrast, here we use a mathematical model to directly interpret thermal measurements in a suite of *in vivo* experiments. In these experiments, we vary several key features such as skin thickness, burn duration, and burn temperature. This approach provides us with a unique opportunity to explore whether the thermal diffusivity and thermal loss depend on skin thickness, burn duration or burn temperature. These details have not been addressed in previous combined studies that make use of both experimental measurements and mathematical models [23].

Examining the relationship between temperature, burn duration and injury severity is essential for guiding scald burn injury prevention standards. Accidental and non-accidental hot tap water scalds may result from exposure to moderate temperature water for long durations [24,25]. One key scald prevention approach is regulating the temperature of hot water delivered by bathroom taps in domestic dwellings, which in many countries is legislated to be no greater than 48 °C [26,27] or 50 °C [28]. For this reason, we focus our experiments on moderate temperature burn conditions (50–60 °C) over relatively long durations (60–600 s). Since we deal with a heat transfer process through a relatively thin layer of skin, and our experiments do not measure spatial differences in temperature within the thin layer of skin, we interpret the experiments using a simplified, depth-averaged, mathematical model that neglects spatial gradients [29,30]. This allows us to develop an exact, closed-form solution of the simplified mathematical model. We calibrate this solution to data from various experimental conditions, providing multiple opportunities to estimate α and the loss rate, k. Our combined experimental and modelling study provides valuable, quantitative information about heat conduction in living skin that cannot be obtained by extrapolating from previous *ex vivo* experiments.

2. Materials and methods

2.1. Animal experiments

A porcine (pig) burn model is chosen because of the anatomical and physiological similarities to human skin [3–7]. Juvenile pigs have a skin thickness of 2–2.3 mm (12 weeks old) [31,32] and 1–1.3 mm (5 weeks old) [6], which closely approximates the skin thickness of a human adult and a human child [33], respectively. All methods conform to the Australian National Health and Medical Research Council published code of practice for animal research. Ethics approval was obtained from the University of Queensland's animal ethics committee (QCMRI/446/15/QCHF), and all animals were treated in a humane manner. Seven female Large White (Yorkshire) juvenile pigs, weighing 27 kg and aged 12 weeks, and two female Large White (Yorkshire) weaner pigs, weighing 10 kg and aged 5 weeks, were used. Pigs were delivered to the animal house seven days prior to commencing the experiment to allow for acclimatisation. Animals were given a standard pellet diet and free access to water, with fasting overnight prior to anaesthesia.

2.1.1. Study protocol

Scald burns were created on the backs of pigs whilst they were under a general anaesthetic. Anaesthesia was induced with Ketamine 13 mg/kg (Ketamine 100 mg/ml Ceva™, Glenorie, NSW, Australia) and 1 mg/kg Xylazine (Ilium Xylazil 100 mg/ml, Ilium™, Troy laboratories Pty Ltd, NSW, Australia) and maintained with Isoflurane (Attane, Bayer, Australia Ltd). Buprenorphine 0.01 mg/kg (Temgesic® 0.3 mg/ml Reckitt Benckiser, Healthcare, UK) was administered peri-operatively to provide analgesia and a transdermal Fentanyl 50 μg/hr patch (Durogesic®50, Janssen-Lilag Pty Ltd, North Ryde, Australia) was applied for post-operative analgesia. The hair on the back and flanks was clipped prior to scald creation. On day seven (endpoint of main experiment) the animals were euthanased with 15 ml of sodium pentobarbitone (Lethabarb™, Virbac Pty Ltd, NSW, Australia).

Eight burns were created on the paravertebral region of each pig, with four burns per side. The burn injury was created by applying a purpose made scald device (Fig. 1). Two different diameter devices were used for the two different age pigs, with a 50 mm diameter for the older animals and a 30 mm diameter device for the younger animals, as the smaller animals have a reduced surface area available for burn creation. Pre-heated water was pumped into the scald device and vacuum suctioned out at an equivalent rate, ensuring a constant level of water within the device at all times. We used a water bath (Grant Instruments, Cambridge, UK) to maintain the water at a constant temperature. Water temperature within the scald device was recorded using a digital 54II Fluke® thermometer (Fluke Australia Pty Ltd., North Melbourne, Australia).

2.1.2. Temperature monitoring

For each experiment the subdermal temperature probe was inserted using a previously described technique [34,35]. The subdermal temperature probe was used to monitor the temperature within the skin during each experiment. Briefly, prior to scalding, a 14 gauge, 2.1 mm by 45 mm cannula was inserted obliquely from outside the marked wound area and advanced under the dermis until the tip was in the centre of the burn area. The stylet was removed and a type K thermocouple (Radiospares Components Pty Ltd., Smithfield, Australia) was inserted and taped into position. A digital 54II Fluke thermometer automatically logged temperature measurements for the initial subdermal temperature, denoted $T(0)$, and then every second after the heated water was applied for

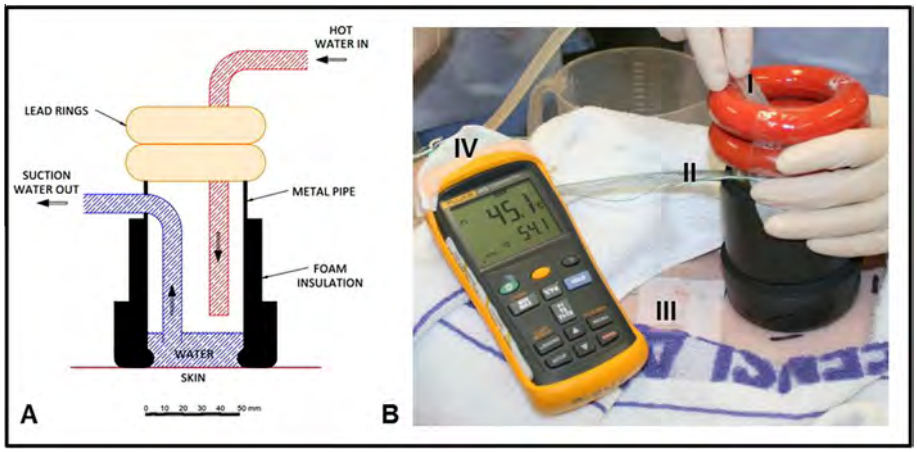

Fig. 1. Scald creation device and subdermal temperature monitoring. The scald creation device consists of a metal pipe covered with insulation tubing and a suction tube. (A) Schematic showing inflow and outflow of hot water in the 50 mm diameter scald creation device. (B) Photograph showing an example of creating a burn where: (I) hot water inflow; (II) suction of water out of the device; (III) insertion point of the subdermal temperature probe; and (IV) shows the Fluke thermometer, where the upper number is the subdermal temperature and the lower number is the temperature of water in the scald creation device.

the shorter burn duration experiments (60–120 s), or every 10 s for the longer burn duration experiments (300–600 s). Subdermal temperature logging was continued for at least 60 s after the heat source was removed, or until a maximum, steady, subdermal temperature was reached. The temperature of the external skin surface was measured at a different site on the same animal using a separate temperature probe. In the 12 week old pigs the following burn conditions were tested: Temperature of the water, $T_w = 50$, 55, and 60 °C, for burn durations of $t_d = 60$ and 120 s, and then $T_w = 50$ and 55 °C, for $t_d = 300$ and 600 s. In the 5 week old pigs, with thinner skin, four burn conditions were tested: $T_w = 50$ °C for $t_d = 60$, 120, 300 and 600 s.

Overall, the experimental programme involved performing fourteen different groups of burns. Each of the fourteen different burn conditions was replicated at least four times, giving a total of sixty four individual burns. The burn conditions included here for analysis were specifically chosen as part of another study to examine clinically mid-deep dermal burns. As such, for $T_w = 60$ °C, a burn duration of $t_d = 120$ s led to a severe full thickness burn injury and additional testing for longer durations was not required. For experiments involving the 5 week old pigs, the range of burn conditions tested was limited, based on ethical approval for younger animals.

2.2. Mathematical modelling

Theoretical studies of heat conduction in biological tissues often invoke Pennes' bioheat equation [12,13,17,36,37]. This partial differential equation describes the variation of temperature in a biological tissue as a function of position and time. Since we measured the temperature at one location within the layer of skin, we do not report any spatial differences in temperature throughout the skin layer. Furthermore, we find that the initial subdermal temperature, $T(0)$, and the external surface temperature of the skin are very similar, and so there is no initial variation in temperature with depth. This observation, combined with the fact that these experiments focus on heat transfer through a relatively thin tissue, motivate us to consider a simplified depth-averaged mathematical model that neglects spatial variations in temperature [29,30]. Accordingly, the experiments are modelled using an ordinary differential equation instead of a partial differential equation.

Assuming the average temperature in the tissue is $T(t)$, the mathematical model governing the dynamics of the experiments can be written as,

$$\frac{dT(t)}{dt} = \frac{\alpha}{H^2}[T_{burn}(t) - T(t)] - k(T(t) - T_{ref}), \tag{1}$$

where t is time, α is the thermal diffusivity, H is the skin thickness, $T_{burn}(t)$ is the temperature of the scald burn applied at the surface, and k is the thermal loss rate. The thermal loss is taken to be proportional to the difference between the average temperature within the tissue and some reference temperature, T_{ref}. Results in Appendix A show how Eq. (1) can be obtained by depth-averaging the Pennes' bioheat equation.

To solve Eq. (1) we must specify $T_{burn}(t)$ and T_{ref}. For all experiments we consider, we model the applied scald burn using

$$T_{burn}(t) = T_w \quad t < t_d, \tag{2}$$

$$T_{burn}(t) = T_s \quad t > t_d,$$

where T_w is the temperature of the water in the scald creation device, t_d is the duration of the burn, and T_s is the surface temperature of the skin. The choice for the form of $T_{burn}(t)$ in Eq. (2) exactly replicates the applied surface temperature for the initial period, $t < t_d$. Setting $T_{burn}(t) = T_s$ in the latter period, $t > t_d$, is an approximation. Our rational for using this approximation is that it correctly models the expected long time behaviour, $T(t) = T_s$ as $t \to \infty$.

We must also specify the reference temperature for the loss term in Eq. (1). Since the initial measured subdermal temperature is very similar to the measured surface temperature, $T(0) \approx T_s$, we assume that $T_{ref} = T_s$. This means that when the heat source is applied and the average temperature in the skin layer increases above the initial temperature, there will be some loss of thermal energy. This loss could represent perfusion into the blood supply [12,13,17,36,37] or to another area of the tissue.

With these assumptions, and writing $\lambda = (\alpha T_w/H^2 + kT_s)/(\alpha/H^2 + k)$ for notational convenience, the solution of Eq. (1) can be written as

$$\begin{aligned} T(t) &= [T_s - \lambda]\exp(-t[\alpha/H^2 + k]) + \lambda, \quad t < t_d, \\ T(t) &= T_s + [T_s - \lambda]\{1 - \exp(t_d[\alpha/H^2 + k])\}\exp(-t[\alpha/H^2 + k]), \quad t > t_d, \end{aligned} \tag{3}$$

To apply Eq. (3) to our experiments we assume that T_w, T_s, t_d and H are either measurable, or are specified as a part of the experimental design. Therefore, the only unknown parameters in the model are α and k. To estimate these two parameters we calibrate Eq. (3) to provide the best match to the experimental measurements of the

subdermal temperature. We use MATLAB's lsqcurvefit routine [38] to provide a least-squares estimate of α and k.

3. Results and discussion

3.1. Experimental results

Data from a total of sixty four burns are used, with at least four replicates for each burn condition. The average thickness of the dermis, H, measured microscopically, is 2.27 ± 0.25 mm in the 12 week old animals, and 1.40 ± 0.14 mm in the 5 week old animals. Based on our experience, we assume that the position of the subdermal probe is directly beneath the dermis, thus the depth of the probe is approximately H. The average initial subdermal temperature $T(0)$, prior to scalding is 34.2 ± 0.8 °C, which is very similar to the average initial external surface temperature of the skin, $T_s = 33.7 \pm 0.9$ °C. This suggests that, at the beginning of the experiment, there is no spatial variation in temperature with depth.

Results for subdermal temperatures are shown in Fig. 2. These results are reported in terms of the average temperature profiles that are obtained by averaging the experimental data across each experimental replicate for each burn condition considered. Overall, the trend is for the subdermal temperature to increase most rapidly when the heat source is first applied. The subdermal temperature then continues to increase, but at a slower rate, for the remainder of the exposure. Once the heat source is removed the temperature decreases. Some of the longer duration burn conditions eventually approach a steady subdermal temperature profile, which has also been reported by others [9]. For example, the experiments with $t_d = 600$ s and $T_w = 50$ °C (Fig. 2D) appear to approach a steady subdermal temperature of approximately 44 °C, after approximately 400 s. This indicates that there must be some loss in the system otherwise the steady subdermal temperature would eventually approach $T_w = 50$ °C. We observe a slightly different trend for the shorter duration burns (60–120 s) since the subdermal temperatures do not appear to reach a steady temperature within the timescale of these shorter experiments.

Similar to others [8,39,40], our results in Fig. 2 indicate some variation between different experimental replicates of the same burn condition. We quantify this variation in terms of the sample standard error. There are two main causes of this variability. Firstly, these are *in vivo* animal experiments, and results are subject to the natural variations in skin structure between animals, and natural variations between different anatomical locations on the same animal. Secondly, although placement of the subdermal probe is performed by the same person, some variation in the probe placement is unavoidable. In particular, it is possible that some probes were placed deeper into the subcutaneous tissue beneath the dermis than others. However, our study is strengthened by including multiple replicates for the same burn condition on different animals at different anatomical locations.

Comparing subdermal temperature profiles in thicker and thinner skinned animals (Fig. 2C–D), indicates that the same burn condition leads to different outcomes. In general, we see the same burn condition applied to a thinner skinned animal leads to higher subdermal temperatures compared to the thicker skinned animals. To further explore these differences we show the magnitude of change in subdermal temperature, $\Delta T(t) = T(t) - T(0)$, for some of these experiments in Fig. 3. For the same burn conditions we observe that the magnitude and rate of increase in subdermal temperature is greatest for thinner skin. To the best of our knowledge, this is the first *in vivo* experimental study demonstrating directly comparable data describing heat conduction in skin of different thickness.

3.2. Modelling results

All experimental measurements for each burn condition were repeated at least four times. The model calibration procedure is applied to each set of replicate data to produce several estimates of α and k for each burn condition. Results in Fig. 4 compare some experimental data to the solution of the calibrated mathematical model. While the calibrated mathematical model does not capture every detail of the experimental data, the key features are broadly replicated.

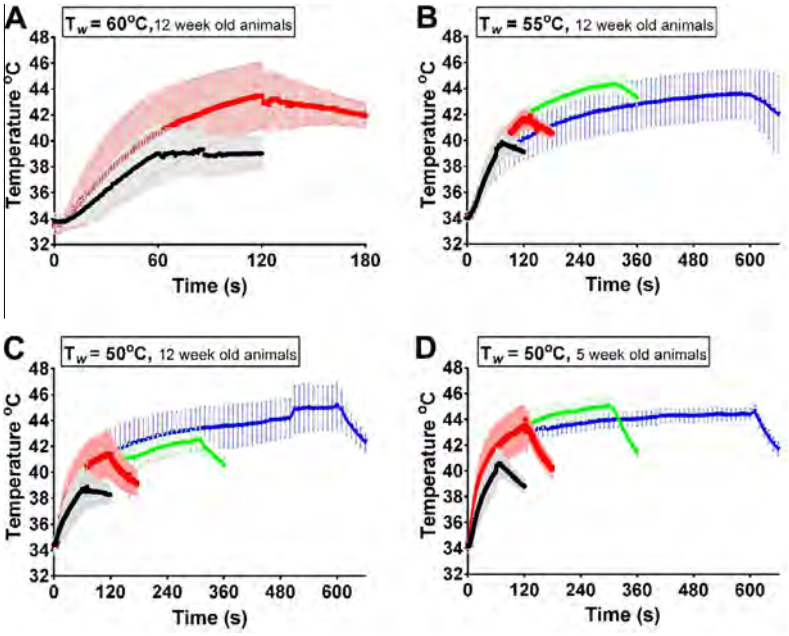

Fig. 2. Averaged subdermal temperature profiles for different burn conditions. Results in A–D correspond to $T_w = 60$, 55 and 50 °C (12 week old pigs), and $T_w = 50$ °C (5 week old pigs), respectively. Different burn durations include: $t_d = 60$ (black); 120 (red); 300 (green); and 600 s (blue). Data points correspond to the sample mean, and the error bars indicate the sample standard error, $\sigma/(n-1)$. (For interpretation of the references to colour in this figure legend, the reader is referred to the web version of this article.)

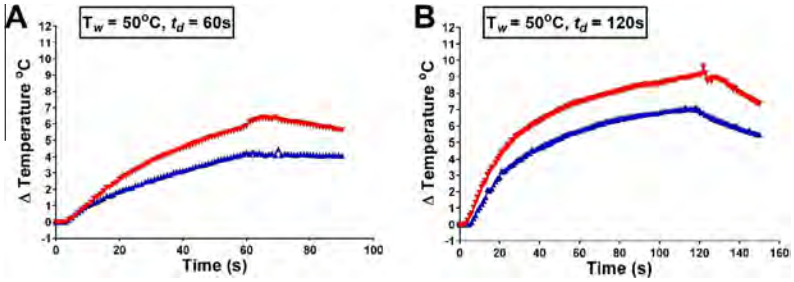

Fig. 3. Average change in subdermal temperature for 50 °C scalds. Data for both 5 week (red) and 12 week (blue) animals are given. Results in A correspond to $t_d = 60$ s, and results in B correspond to $t_d = 120$ s. (For interpretation of the references to colour in this figure legend, the reader is referred to the web version of this article.)

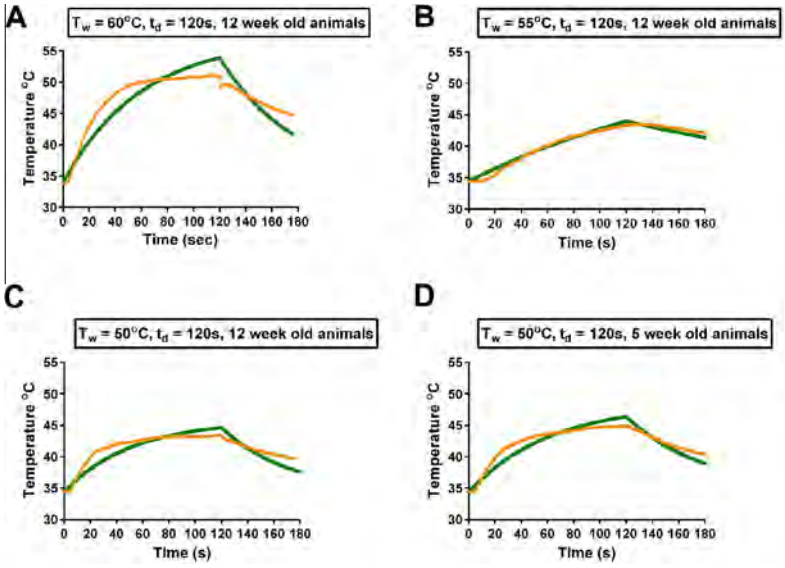

Fig. 4. Comparison of experimental data for a single experimental replicate to the solution of the calibrated mathematical model for four different burn conditions. Results in A–D correspond to $T_w = 60$, 55, 50 °C (12 week old animals) and $T_w = 50$ °C (5 week old animals), respectively. In all cases the experiments correspond to $t_d = 120$ s. Each plot compares the *in vivo* experimental data (orange) with the solution of the calibrated mathematical model (green). (For interpretation of the references to colour in this figure legend, the reader is referred to the web version of this article.)

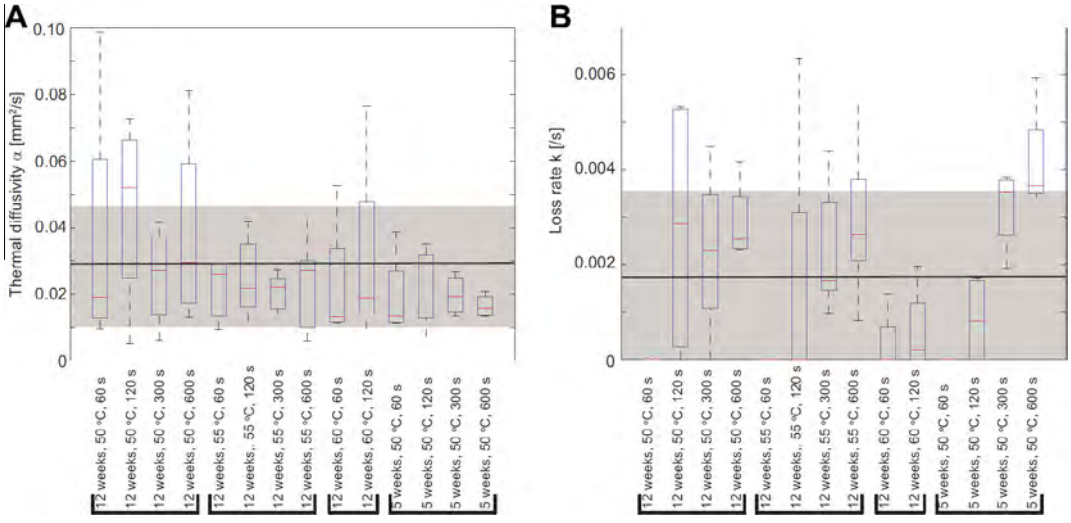

Fig. 5. Boxplots showing estimates of α and k for all burn conditions. The boxplots are created with MATLAB [38]. The solid black horizontal lines indicate the sample mean across all experimental burn conditions, and the grey shaded region indicates the mean ± one sample standard deviation to illustrate the variability across all experimental conditions. Results in A show estimates of the thermal diffusivity, the sample mean is $\alpha = 0.027$ mm^2/s and the sample standard deviation is 0.020 mm^2/s. Results in B show estimates of the loss rate, the sample mean is $k = 0.00170$/s and the sample standard deviation is 0.00186/s.

Results summarizing estimates of α and k for the fourteen different groups of experiments are shown in Fig. 5. Averaging the estimates of α and k across all fourteen groups of experiments gives $\alpha = 0.03 \pm 0.02$ mm^2/s (to one significant figure), and $k = 0.002 \pm 0.002$/s (to one significant figure), where the variability is given by the sample standard deviation. Visual inspection of the results for the thermal diffusivity (Fig. 5A) indicates that the majority of estimates of α for each experimental group lie within one standard deviation about the mean. Since there appears to be no discernible trend in the mean estimates of α for varying burn duration, burn temperature and skin thickness, it is reasonable to characterize α using a constant for all experimental scenarios considered.

Results for the loss rate (Fig. 5B) indicate that the variability between estimates of k between different groups of experiments is greater than the variability of α between different groups of experiments. Our results suggest that the thermal loss plays an insignificant role in short duration burn conditions, whereas our estimates of k are larger for the longer duration burn conditions. It is difficult to speculate about the reason for this, however it is possible that for longer duration exposures ($\geqslant$ 300 s), there is an increase in the rate of heat loss to the blood supply. In response to heat exposure, vessels in the local tissue area may dilate, increasing blood perfusion and enhancing heat dissipation. Increased perfusion to the local tissue and surrounding tissue may take several minutes to reach maximal effect.

Our estimates of α allow us to predict the approximate amount of time required for the thermal energy to propagate vertically down, through the skin, as H^2/α. For the 12 week old animals, with $\alpha = 0.03$ mm^2/s and $H = 2.27$ mm, the time taken will be approximately 170 s. Whereas, for the 5 week old animals, with $H = 1.40$ mm, the time taken will be approximately 70 s.

Our average estimate of α is approximately 3–10 times smaller than previously reported *in vivo* estimates from 1947 [8]. There are several possible explanations for this difference. A key difference between our experiments and those of Henriques and Moritz [8] is that we directly measure the transfer of thermal energy vertically down, through a layer of skin. In contrast, Henriques and Moritz measure the caloric uptake of skin, and then convert this quantity into an estimate of thermal diffusivity by making assumptions about the density and thermal conductivity of the skin. Another important difference is in the experimental design. Henriques and Moritz [8] create a burn using a heated copper disk, whereas we create scald burns using hot water. Furthermore, advances in technology now us to use modern, calibrated and reproducible measurement instrumentation, whereas the previous results from 1947 relied on custom-made measuring instruments.

4. Conclusions

In this work we consider a series of scald burns in an *in vivo* porcine model. We choose to work with a porcine model because pig skin is anatomically and physiologically similar to human skin [3–5]. Our experimental design allows for the collection of high quality *in vivo* data, with multiple replicates performed on different animals, and at different anatomical locations for the same burn condition. Here, we examine how the thermal properties of skin depend on burn duration, burn temperature, and skin thickness. It is important to consider these variables because thermal injuries may occur under many different conditions. To the best of our knowledge, the experimental data set presented here is the first *in vivo* study to directly compare heat conduction in thin and thick skin (representative of a human child and adult skin) subject to the same burn conditions.

To provide additional quantitative insight into our experimental data set we also interpret our data with a mathematical model. In particular, the focus of using the mathematical model is to provide estimates of the thermal diffusivity and the thermal loss rate, and to explore whether these estimates depend on burn duration, burn temperature or skin thickness. Our overall estimates are $\alpha = 0.03$ mm^2/s and $k = 0.002$/s (to one significant figure). For long duration, moderate temperature burns, our estimates of α appear to be independent of the burn duration, burn temperature and skin thickness. In contrast, our estimates of k are more variable. The model calibration procedure suggests that there is virtually no thermal loss during the very short time burn duration experiments whereas a larger loss rate is relevant for the longer duration burn conditions.

Both experiments and modelling suggest avenues for future research. Future experiments may include multiple temperature measurements at different depths, which would allow for a greater understanding of how heat is transferred through the different layers of the skin. In particular, whether heat transfer may change at different dermal depths and potentially affect the predicted time required to create a deep dermal versus a superficial dermal burn. Additionally, placement of the temperature probe using ultrasound guidance could be used, which would also enable *in vivo* quantification of probe depth. Further investigations regarding the thermal loss rate and the role of blood perfusion could also be studied by repeating experiments on skin with no blood perfusion (non-living tissue). Extensions of our modelling framework could include spatial effects, but this would require additional experimental data.

Our estimates of α can be applied with most confidence to inform modelling studies of heat transfer where skin is exposed to moderate temperatures for relatively long durations, similar to the experimental procedure presented here. For example, this could include burn prevention strategies [20,41,42], predicting thermal damage for accidents [43], forensic medicine [29,30] and thermal therapy studies [44]. Importantly, improving understanding of temperature conduction in the skin is a vital first step towards examining the relationship between heat conduction and tissue damage, which has significant clinical applications. Furthermore, all data used in our mathematical model calibration procedure is available for re-use in future studies (Supplementary Material). This could be useful to enhance experimental design and to minimise animal use.

The data and modelling presented in this paper are part of a broader study investigating the pathophysiology of burns. The mathematical modelling completed on this simplified dataset enables an initial examination of the complex process of heat conduction in living skin and further work examining the relationship between heat conduction and tissue damage is currently underway. Overall, our study highlights how collaboration between researchers with expertise in animal/laboratory based experimental studies and theoreticians who specialize in applying mathematical models to interpret biological or clinical data can enrich the overall value of results obtained.

Acknowledgements

MJS appreciates support from the Australian Research Council (FT130100148, DP14100249). LC appreciates support from the National Health and Medical Research Council (APP1035907). We thank Emeritus Professor Sean McElwain for providing comments on a draft version of this manuscript, and we thank the two anonymous referees for providing helpful comments.

Appendix A. Approximate mathematical model

We begin by considering the conduction of heat in a one-dimensional tissue, of thickness H. Assuming that the transport

of energy is driven by linear conduction, and there is a loss of thermal energy by some mechanism, such as perfusion, conservation of energy arguments lead to

$$\frac{\partial T^*(x,t)}{\partial t} = \alpha \frac{\partial^2 T^*(x,t)}{\partial x^2} - k(T^*(x,t) - T_{ref}), \tag{5}$$

on $0 < x < H$, where $T^*(x,t)$ is the temperature at position x and time t, α is the thermal diffusivity and k is the loss rate. In this model, we adopt a standard approach by assuming that thermal losses are proportional to the difference between the local temperature, $T^*(x,t)$, and some reference temperature, T_{ref}. In many applications the loss term is thought to represent the transfer of energy into the blood supply and the reference temperature is taken to be the temperature of the blood [12,45].

Since we deal with a relatively thin layer of skin, and our experimental measurements do not report spatial differences in temperature within the layer of skin, we simplify Eq. (5) by averaging $T^*(x,t)$ vertically across the depth of the layer to give

$$T(t) = \frac{1}{H}\int_0^H T^*(x,t)\, dx, \tag{6}$$

so that $T(t)$ represents the spatially-averaged temperature within the tissue layer [44]. To simplify Eq. (5) we divide both sides by H and integrate from $x = 0$ to $x = H$. Treating α, k, and T_{ref} as constants, we obtain

$$\frac{dT(t)}{dt} = \frac{\alpha}{H}\left[\frac{\partial T^*(H,t)}{\partial x} - \frac{\partial T^*(0,t)}{\partial x}\right] - k(T(t) - T_{ref}). \tag{7}$$

If we further assume that the flux of thermal energy at the lower boundary, where $x = H$, is negligible, and we approximate the temperature gradient at the upper boundary, where $x = 0$, as $\frac{\partial T^*(0,t)}{\partial x} \approx \frac{T(t) - T_{burn}(t)}{H}$, we obtain

$$\frac{dT(t)}{dt} = \frac{\alpha}{H^2}[T_{burn}(t) - T(t)] - k(T(t) - T_{ref}), \tag{8}$$

This is a simplified ordinary differential equation that describes the dynamics of the average temperature of the layer of skin. We note that many practical applications of mathematical models of heat transfer processes in real biological tissues use spatially-averaged models rather than spatial models. The motivation for the use of such spatially-averaged models is that even relatively sophisticated experimental measurements may not resolve spatial temperature differences sufficiently to warrant the application of a full spatial model [29,30].

Appendix B. Supplementary data

Supplementary data associated with this article can be found, in the online version, at http://dx.doi.org/10.1016/j.ijheatmasstransfer.2016.05.070.

References

[1] R. Rayner, J. Prentice, Paediatric burns: a brief global review, Wound Practice Res. 19 (1) (2011) 39–46.
[2] K.M. Bombaro, L.H. Engrav, G.J. Carrougher, S.A. Wiechman, L. Faucher, B.A. Costa, D.M. Heimbach, F.P. Rivara, S. Honari, What is the prevalence of hypertrophic scarring following burns?, Burns 29 (4) (2003) 299–302
[3] A. Abdullahi, S. Amini-Nik, M. Jeschke, Animal models in burn research, Cell. Mol. Life Sci. 71 (17) (2014) 3241–3255.
[4] W. Meyer, R. Schwarz, K. Neurand, The skin of domestic mammals as a model for the human skin, with special reference to the domestic pig, Curr. Probl. Dermatol. 7 (1978) 39–52.
[5] W. Montagna, J.S. Yun, The skin of the domestic pig, J. Invest. Dermatol. 42 (1964) 11–21.
[6] A.R. Moritz, F.C. Henriques, Studies of thermal injury: II. The relative importance of time and surface temperature in the causation of cutaneous burns, Am. J. Pathol. 23 (5) (1947) 695–720.
[7] T.P. Sullivan, W.H. Eaglstein, S.C. Davis, P. Mertz, The pig as a model for human wound healing, Wound Repair Regen. 9 (2) (2001) 66–76.
[8] F.C. Henriques, A.R. Moritz, Studies of thermal injury: I. The conduction of heat to and through skin and the temperatures attained therein. A theoretical and an experimental investigation, Am. J. Pathol. 23 (4) (1947) 530–549.
[9] M.A. El-Brawany, D.K. Nassiri, G. Terhaar, A. Shaw, I. Rivens, K. Lozhken, Measurement of thermal and ultrasonic properties of some biological tissues, J. Med. Eng. Technol. 33 (3) (2009) 249–256.
[10] S.M. Brown, M.L. Baesso, J. Shen, R.D. Snook, Thermal diffusivity of skin measured by two photothermal techniques, Anal. Chim. Acta 282 (3) (1993) 711–719.
[11] H.H. Pennes, Analysis of tissue and arterial blood temperatures in the resting human forearm. 1948, J. Appl. Physiol. (1985), 85(1) (1998) 5–34.
[12] E. Kengne, A. Lakhssassi, Bioheat transfer problem for one-dimensional spherical biological tissues, Math. Biosci. 269 (2015) 1–9.
[13] K.R. Diller, L.J. Hayes, G.K. Blake, Analysis of alternate models for simulating thermal burns, J. Burn Care Rehab. 12 (2) (1991) 177–189.
[14] H.S. Carslaw, J.C. Jaeger, Conduction of Heat in Solids, Clarendon Press, Oxford, 1959.
[15] J. Crank, The Mathematics of Diffusion, Clarendon Press, 1979.
[16] J. Liu, X. Chen, L.X. Xu, New thermal wave aspects on burn evaluation of skin subjected to instantaneous heating, IEEE Trans. Biomed. Eng. 46 (4) (1999) 420–428.
[17] B.L. Viglianti, M.W. Dewhirst, J.P. Abraham, J.M. Gorman, E.M. Sparrow, Rationalization of thermal injury quantification methods: application to skin burns, Burns 40 (5) (2014) 896–902.
[18] A. Baldwin, J. Xu, D. Attinger, How to cool a burn: a heat transfer point of view, J. Burn Care Res. 33 (2) (2012) 176–187.
[19] S.C. Jiang, N. Ma, H.J. Li, X.X. Zhang, Effects of thermal properties and geometrical dimensions on skin burn injuries, Burns 28 (8) (2002) 713–717.
[20] N. Johnson, J. Abraham, Z. Helgeson, Calculations of scald burns: effects of water temperature, exposure duration, and clothing, in: ASME 2010 International Mechanical Engineering Congress and Exposition, American Society of Mechanical Engineers, 2010, pp. 199–208.
[21] D.P. Orgill, M.G. Solari, M.S. Barlow, N.E. O'Connor, A finite-element model predicts thermal damage in cutaneous contact burns, J. Burn Care Res. 19 (3) (1998) 203–209.
[22] J.H. Cantrell Jr., Ultrasonic determination of thermodynamic threshold parameters for irreversible cutaneous burns, J. Acoust. Soc. Am. 72 (2) (1982) 337–339.
[23] J.Y. Lee, S.N. Jung, H. Kwon, In vitro burn model illustrating heat conduction patterns using compressed thermal papers, Wound Repair Regen. 23 (1) (2015) 124–131.
[24] S. Daria, N.F. Sugar, K.W. Feldman, S.C. Boos, S.A. Benton, A. Ornstein, Into hot water head first: distribution of intentional and unintentional immersion burns, Pediatr. Emerg. Care 20 (5) (2004) 302–310.
[25] M.O. Titus, A.L. Baxter, S.P. Starling, Accidental scald burns in sinks, Pediatrics 111 (2) (2003) E191–194.
[26] The Building Regulations 2010 (SI 2010/2214), Part G; Sanitation, Hot Water Safety and Water Efficiency, pp. 18–26.
[27] M. Peck, A.C. Brewer, M. Pressman, E. Blank, A. Mickalide, Hot tap water legislation in the United States, J. Burn Care Res. 31 (6) (2010) 918–925.
[28] Australian/New Zealand Standard 3500.4: 2003 Plumbing and Drainage Part 4: Heated water services, pp. 9–11.
[29] M.R. Rodrigo, Time of death estimation from temperature readings only: a Laplace transform approach, Appl. Math. Lett. 39 (2015) 47–52.
[30] M.R. Rodrigo, A nonlinear least squares approach to time of death estimation via body cooling, J. Forensic Sci. 61 (2016) 230–233.
[31] U. Henze, A. Lennartz, B. Hafemann, C. Goldmann, C.J. Kirkpatrick, B. Klosterhalfen, The influence of the C1-inhibitor BERINERT and the protein-free haemodialysate ACTIHAEMYL20% on the evolution of the depth of scald burns in a porcine model, Burns 23 (6) (1997) 473–477.
[32] S.Y. Sheu, W.L. Wang, Y.T. Fu, S.C. Lin, Y.C. Lei, J.H. Liao, N.Y. Tang, T.F. Kuo, C.H. Yao, The pig as an experimental model for mid-dermal burns research, Burns 40 (8) (2014) 1679–1688.
[33] S. Seidenari, G. Giusti, L. Bertoni, C. Magnoni, G. Pellacani, Thickness and echogenicity of the skin in children as assessed by 20-MHz ultrasound, Dermatology 201 (3) (2000) 218–222.
[34] L. Cuttle, M. Kempf, O. Kravchuk, G.E. Phillips, J. Mill, X.Q. Wang, R.M. Kimble, The optimal temperature of first aid treatment for partial thickness burn injuries, Wound Repair Regen. 16 (5) (2008) 626–634.
[35] L. Cuttle, M. Kempf, P.Y. Liu, O. Kravchuk, R.M. Kimble, The optimal duration and delay of first aid treatment for deep partial thickness burn injuries, Burns 36 (5) (2010) 673–679.
[36] D. Van de Sompel, T.Y. Kong, Y. Ventikos, Modelling of experimentally created partial-thickness human skin burns and subsequent therapeutic cooling: a new measure for cooling effectiveness, Med. Eng. Phys. 31 (6) (2009) 624–631.
[37] E.Y. Ng, L.T. Chua, Comparison of one- and two-dimensional programmes for predicting the state of skin burns, Burns 28 (1) (2002) 27–34.
[38] Mathworks, 2012 Image Acquisition Toolbox. Users Guide R2012b, in: http://au.mathworks.com/products/matlab/.
[39] V. Jandera, D.A. Hudson, P.M. De Wet, P.M. Innes, H. Rode, Cooling the burn wound: evaluation of different modalities, Burns 26 (3) (2000) 265–270.
[40] M. Kaczmarek, A. Nowakowski, A. Renkielska, J. Grudzinski, W. Stojek, Investigation of skin burns basing on active thermography, in: Proceedings of the 23rd Annual International Conference of the Ieee Engineering in

Medicine and Biology Society, Building New Bridges at the Frontiers of Engineering and Medicine, vol. 1–4, 2001, pp. 2882–2885.
[41] J.P. Abraham, B. Plourde, L. Vallez, J. Stark, K.R. Diller, Estimating the time and temperature relationship for causation of deep-partial thickness skin burns, Burns 41 (8) (2015) 1741–1747.
[42] K.R. Dille, Adapting adult scald safety standards to children, J. Burn Care Res. 27 (3) (2006) 314–322. discussion 323-314.
[43] G.N. Mercer, H.S. Sidhu, A heat transfer model describing burns to the skin from automotive airbags, Aust. New Zealand Ind. Appl. Math. J. 47 (2006) 16.
[44] S. Mahjoob, K. Vafai, Analytical characterization of heat transport through biological media incorporating hyperthermia treatment, Int. J. Heat Mass Transfer 52 (5) (2009) 1608–1618.
[45] M.J. Simpson, Depth-averaging errors in reactive transport modeling, Water Resour. Res. 45 (2) (2009) W02505.